SCIENCE CHINA
Technological Sciences

May 2011 Vol.54 No.5: 1113–1120
doi: 10.1007/s11431-011-4354-8

Passive vibration control of truss-cored sandwich plate with planar Kagome truss as one face plane

GUO Xu & JIANG Jun*

MOE Key Laboratory of Strength and Vibration, Xi'an Jiaotong University, Xi'an 710049, China

Received January 2, 2011; accepted February 16, 2011; published online March 31, 2011

Kagome based high authority shape morphing structure is a kind of truss-cored sandwich metal plate with a planar Kagome truss as one of its face plane. The planar Kagome truss can achieve arbitrary in-plane nodal displacements with minimal internal resistance when its rods are deformed. Moreover, the in-plane deflection of the planar Kagome truss may induce the lateral deflection of the whole sandwich plate. In this paper, the feasibility to enhance the damping of the truss-cored sandwich plate through the replacement of a very small portion of rods in the planar Kagome truss by cylindrical viscoelastic dampers is exploited. The Biot model is chosen to simulate the behavior of the viscoelastic material in the dampers, and the fraction of axial modal strain energy of the rods in the planar Kagome truss is adopted as the index to decide the positions of the dampers. Through complex modal analysis and time-domain simulation, it is shown that the passive vibration control approach is very effective for the vibration reduction of this kind of truss-cored sandwich plates.

truss-cored sandwich plate, passive vibration control, cylindrical viscoelastic damper, modal strain energy

Citation: Guo X, Jiang J. Passive vibration control of truss-cored sandwich plate with planar Kagome truss as one face plane. Sci China Tech Sci, 2011, 54: 1113–1120, doi: 10.1007/s11431-011-4354-8

1 Introduction

Ultra-light-weighted and multi-functional truss-cored metal structure consisting of periodic truss cores and solid face sheets has emerged recently with the advanced manufacturing techniques and is regarded as the new generation of advanced light weight, high strength material. This novel structure is characterized with excellent mechanical performance such as ultra-light, high strength ratio, high stiffness ratio, and possesses multi-functions, such as energy absorption, damping, permeability, heat insulation, heat dispersion, oxidation resistance, electromagnetic screening etc. Truss-cored metal structure is expected to have potential application in astronautics, aviation, ship, automobile, high-speed train and so on.

The Kagome based high authority shape morphing structure (or Kagome structure for short) [1] is a kind of truss-cored sandwich plate. In contrast to other truss-cored sandwich plates that have two solid face sheets, one face sheet of the Kagome structure is replaced by a planar Kagome truss while the other face sheet is still a solid one. The truss-core is a tetrahedral truss that lies in between the two face sheets (see Figure 1). The ancient planar Kagome basket weave pattern truss is simultaneously static determinacy and stiff [2]. This feature of the planar Kagome truss enables its truss rods to be actuated in order to achieve arbitrary in-plane nodal displacements with minimal internal resistance even when their joints are welded. Besides, the 120° symmetry of planar Kagome truss ensures the in-plane elastic isotropy. Moreover, the planar Kagome truss has an optimal weight in comparison with other planar trusses in a specified strength or stiffness.

For the Kagome structure, if some specific rods in the

*Corresponding author (email: jun.jiang@mail.xjtu.edu.cn)

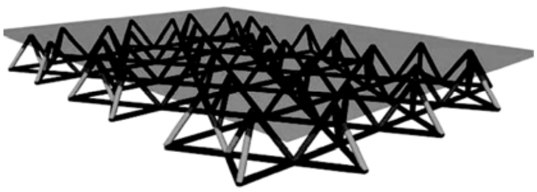

Figure 1 Schematic representation of the Kagome structure [1]. The solid face sheet is shown in dark grey, the core in grey and the planar Kagome truss as one face plane in black.

planar Kagome truss are replaced by linear actuators, transverse displacement of the solid face sheet can be realized only by the in-plane tension-compression actuation forces [1, 3]. The Kagome structure also has excellent resistance to yielding and buckling.

The damping property is an important factor to be considered for the engineering application of metal structural components since various excitations exist in the working environment. Passive vibration control with the use of damping materials is widely adopted in the engineering areas due to the simplicity for implementation and the high reliability. A traditional approach to passively suppress vibration of plate-like structure is using constrained layer damping [4], where the damping layer deforms in shear so as to dissipate vibration energy in a relatively efficient way. Higher damping ratios can also be achieved over a broad range of temperatures and frequencies through the use of multi-damping layers. However, this way of the damping enhancement is at the expense of adding considerable weight and thickness to the original plate and poses a serious limitation to their practical use. For the vibration control of a kind of sandwich structure—honeycomb sandwich plates, Woody and Smith [5] placed energy absorbing foam in the honeycomb pockets to add passive damping.

The multi-functional characters owed by the ultra-light -weighted truss-cored metal sandwich plates may inspire new ideas in vibration control by utilizing their special structural configurations. For the Kagome structure studied in this paper, the character that axial deformation of the rods in the planar Kagome truss can induce the lateral deformation of the sandwich plate will be taken for the passive vibration control. The idea is that a very small portion of the rods in the planar Kagome truss will be replaced by cylindrical viscoelastic dampers. When the Kagome structure is subject to the out-of-plane excitation and undertakes lateral vibration, the cylindrical dampers in the planar Kagome truss will dominantly suffer axial deformation. Since the axial deformation of the cylindrical dampers will cause the shear deformation of the viscoelastic material in the dampers due to the special design configuration, the lateral vibration energy of the sandwich plate will be partially dissipated. Undoubtfully, the effective enhancement of the damping capability of the Kagome structure may promote its potential engineering application.

To verify the feasibility of the above idea, the finite element method is used in this paper. Emphasis is laid on the building of a realistic dynamic model for the cylindrical viscoelastic damper and the optimal placement of the cylindrical dampers, which takes only a very small fraction of the total number of the rods in the planar Kagome truss. The paper is arranged as follows. After the introduction of the Kagome structure and its finite element model in section 2, the dynamic model of the cylindrical damper is built by using the Biot method to describe the viscoelastic material in section 3. Fraction of axial modal elastic strain energy is chosen as an effectiveness index to decide the placement position of the dampers in the planar Kagome truss in section 4. The effectiveness of the passive vibration control is demonstrated by the complex modal analysis and the simulation of time domain response of the Kagome structureunder a broad-bandwidth excitation in section 5. Finally, conclusions are drawn in section 6.

2 Finite element model of Kagome structure

The Kagome (based high authority shape morphing) structure consists of a solid face sheet and a tetrahedral core and a planar Kagome truss as the back-plane (see Figure 1). The solid sheet is made from aluminum alloy and the truss members of the core and the Kagome back-plane are made from stainless steel in the same size. The material parameters and sizes of each part are listed in Table 1. There are total 1584 truss rods of the planer Kagome truss in the Kagome structure studied in this paper.

The commercial software MSC.PATRAN is used to build the finite element model of the Kagome structure which is shown in Figure 2. The face sheet used is discretized by plate element CQUAD4, while the members of the truss-core and planar Kagome truss are modeled by simple beam element CBAR. Both the solid face sheet and the Kagome back plane of the structure are clamped.

The first six natural frequencies of the Kagome structure are computed by MSC.NASTRAN and listed in the first row of Table 1. Assuming that the damping of the structure is of Rayleigh type and the modal damping ratios of both the first and second modes are 1%, we can determine the coefficients α and β from the following formula:

Table 1 Material parameters and size of face sheet and truss rods

Face sheet		Core truss and Kagome truss	
Material	Al alloy	Material	Stainless steel
Young's modulus	73.1 GPa	Young's modulus	193 GPa
Density	2700 kg/m^3	Density	8030 kg/m^3
Length	1.58 m	Truss length	51 mm
Width	1.50 m	Section type	Circle
Depth	1.53 mm	Radius	1.275 mm

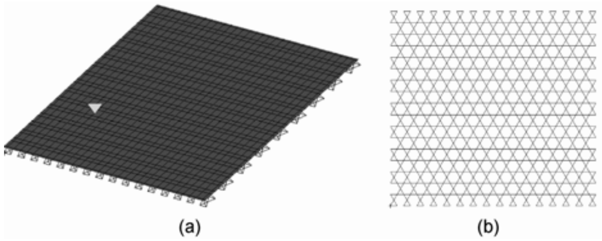

Figure 2 (a) Finite element model of Kagome structure, the triangular represents the observing point of structure response below; (b) the plane of the Kagome structure with a planar Kagome truss.

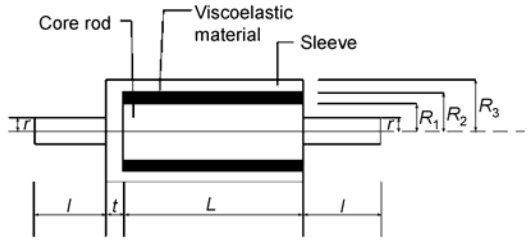

Figure 3 Sketch of the cylindrical sandwich shearing viscoelastic damper. The parameters are given as L=29 mm, t=2 mm, l=10 mm, r=3 mm, R_1=8 mm, R_2=10 mm, R_3=12.4 mm.

$$\xi_i = \frac{1}{2}\left(\frac{\alpha}{\omega_i} + \beta\omega_i\right). \tag{1}$$

We can get α=9.6208 and β=9.4735×10^{-6}. So the 3rd to 6th modal damping ratios can be determined from eq. (1). The modal damping ratios of the first six modes are list in the second row of Table 2.

3 The dynamic model of cylindrical dampers

With the motivation to enhance damping capability of the Kagome structure through the replacement of a very small portion of the members in the planar Kagome truss, the model of the dampers is first built. According to the feature of the planar Kagome truss, the cylindrical sandwich shearing viscoelastic damper [6] with the same length as the truss members is adopted. This kind of damper is a bi-shearing sandwich structure composed of a core rod, a sleeve and viscoelastic material (see Figure 3). When the relative movement between the core rod and the sleeve undergoes, the viscoelastic material will undertake shearing deformation and dissipate energy. To ensure the load applied on the damper to be in the axial direction, the spherical hinges must be used in the connection between the damper and the truss members in order to avoid bending and torsion moments.

To set up a dynamic model of the cylindrical damper that is suitable for incorporation into the finite element model of the Kagome structure, the theory of linear viscoelasticity [7] is used and the constitutive relation for a viscoelastic material can be written as

$$\sigma(t) = G(t)\varepsilon(0) + \int_0^t G(t-\tau)\frac{\mathrm{d}\varepsilon(\tau)}{\mathrm{d}\tau}\mathrm{d}\tau, \tag{2}$$

where σ is stress and ε represents strain. $G(t)$ is material relaxation function. This stress relaxation represents energy loss from the material.

Take Laplace transform on eq. (2) yields

$$\sigma(s) = sG(s)\varepsilon(s), \tag{3}$$

where $sG(s)$ is called material modulus function.

A traditional and widely used method—modal strain energy (MSE) method [8]—is an approximate method by using real modes instead of complex modes, and can reflect the frequency-dependent character of viscoelastic material loss factor. However, the MSE method is restricted to the problem of sinusoidal forcing. That is, it can not simulate the correct viscoelastic behavior across a wide spectrum of frequency. So, over the years, some new methods appeared. Bagley and Torvik [9] developed a fractional derivative model for viscoelastic materials. This method is superior in exactly simulating the viscoelastic behavior but impractical in being put into system motion equations because the matrices become too large. This drawback restricts the use of this method in practice. The augmenting thermodynamic fields (ATF) method [10] and its extended form, an elastic displacement fields (ADF) method [11], were put forward by Lesieutre and his coworkers. These methods considered viscoelastic properties by adding additional coordinates called dissipation coordinates to account for the frequency and temperature dependence of this kind of material. The ATF and ADF method can be extended to adapt the finite element method easily. The Golla-Hughes-McTavish (GHM) [12] method utilized the dissipation coordinates like ATF/ADF method. In contrast, the GHM approach internalizes the dissipation variables at the element level while in the ATF/ADF method these variables are conceptualized over the whole structure. Unlike these methods, the dissipation coordinates of GHM method participate in the element mass matrix so a conventional second-order structural model can be assembled.

Biot method is a method, like the ATF/ADF and GHM methods, still using the concept of dissipation coordinates [13]. It is sometimes referred to as the first order version of GHM method [14] because this method is similar to GHM approach but the additional coordinates do not participate in element mass matrix. Owing to this feature, the system equation by using Biot method is simpler.

Table 2 The natural frequencies and modal damping ratios of the first six modes of the Kagome structure

Mode#	1	2	3	4	5	6
Frequency (Hz)	118	218	232	318	356	389
Modal damping ratio (%)	1.00	1.00	1.02	1.19	1.28	1.35

With the Biot model, the modulus function of viscoelastic material can be written as a series of terms called mini-oscillator terms:

$$sG(s) = G^{\infty}\left(1+\sum_{k=1}^{n} a_k \frac{s}{s+b_k}\right). \tag{4}$$

The factor G^{∞} represents the equilibrium value of the modulus, the final value of the relaxation function $G(t)$. $\{a_k, b_k\}$ are positive constant determined by the shape of modulus function in the Laplace domain, k=1, 2, $\cdots$, n, while n is the total number of mini-oscillator terms. Figure 4 illustrates the mechanical analogy of Biot model.

In ref. [15] the finite element model of the dynamic equation of viscoelastic material by n mini-oscillator terms was written as

$$\hat{\boldsymbol{M}}\ddot{\boldsymbol{q}} + \hat{\boldsymbol{C}}\dot{\boldsymbol{q}} + \hat{\boldsymbol{K}}\boldsymbol{q} = \hat{\boldsymbol{f}}, \tag{5}$$

where $\boldsymbol{q} = \{\boldsymbol{x} \quad z_1 \quad \cdots \quad z_m\}^{\mathrm{T}}$ is the variable vector and $\boldsymbol{x}$ represents the displacement vector of the damper, which is governed by the dynamical equation

$$\boldsymbol{M}\ddot{\boldsymbol{x}} + \boldsymbol{K}\left(\boldsymbol{G}(t)\boldsymbol{x}(0) + \int_0^t \boldsymbol{G}(t-\tau)\dot{\boldsymbol{x}}\mathrm{d}\tau\right) = \boldsymbol{F}, \tag{6}$$

where $\boldsymbol{M}$ and $\boldsymbol{K}$ are the mass and stiffness matrices of the damper. $z_1, \cdots, z_n$ are the so-called dissipation coordinates. $\hat{\boldsymbol{f}} = \{\boldsymbol{F} \quad 0 \quad \cdots \quad 0\}^{\mathrm{T}}$ is the force vector. The symmetric coefficient matrices in eq. (5) are given as

$$\hat{\boldsymbol{M}} = \begin{bmatrix} \boldsymbol{M} & 0 & \cdots & 0 \\ 0 & 0 & \cdots & 0 \\ \vdots & \vdots & \ddots & \vdots \\ 0 & 0 & \cdots & 0 \end{bmatrix}, \quad \hat{\boldsymbol{C}} = \begin{bmatrix} 0 & 0 & \cdots & 0 \\ 0 & \dfrac{a_1\boldsymbol{\Lambda}}{b_1} & \cdots & 0 \\ \vdots & \vdots & \ddots & \vdots \\ 0 & 0 & \cdots & \dfrac{a_m\boldsymbol{\Lambda}}{b_m} \end{bmatrix},$$

$$\hat{\boldsymbol{K}} = \begin{bmatrix} \boldsymbol{K}\left(1+\sum\limits_{k=1}^{m} a_k\right) & -a_1\boldsymbol{Q} & \cdots & -a_m\boldsymbol{Q} \\ -a_1\boldsymbol{Q}^{\mathrm{T}} & a_1\boldsymbol{\Lambda} & \cdots & 0 \\ \vdots & \vdots & \ddots & \vdots \\ -a_m\boldsymbol{Q}^{\mathrm{T}} & 0 & \cdots & a_m\boldsymbol{\Lambda} \end{bmatrix}, \tag{7}$$

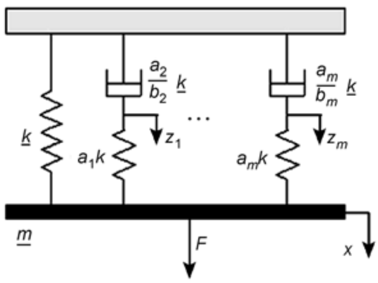

Figure 4 The mechanical analogy of Biot model [13].

with

$$\boldsymbol{K} = G^{\infty}\bar{\boldsymbol{K}}, \quad \bar{\boldsymbol{K}} = \bar{\boldsymbol{Q}}\bar{\boldsymbol{\Lambda}}\bar{\boldsymbol{Q}}^{\mathrm{T}}, \quad \boldsymbol{\Lambda} = G^{\infty}\bar{\boldsymbol{\Lambda}}, \quad \boldsymbol{Q} = G^{\infty}\bar{\boldsymbol{Q}}\bar{\boldsymbol{\Lambda}}, \tag{8}$$

where $\bar{\boldsymbol{\Lambda}}$ is a diagonal matrix of the nonzero eigenvalues of matrix $\bar{\boldsymbol{K}}$, and the corresponding normalized eigenvectors form the columns of matrix $\bar{\boldsymbol{Q}}$.

The cylindrical damper shown in Figure 3 can be regarded as a system with two degrees of freedom. The mass and stiffness matrices in eq. (6) can be defined as

$$\boldsymbol{M} = \begin{bmatrix} m_c & \\ & m_s \end{bmatrix}, \quad \boldsymbol{K} = \frac{2\pi R_2 L}{R_2 - R_1}\begin{bmatrix} 1 & -1 \\ -1 & 1 \end{bmatrix}, \tag{9}$$

where m_c and m_s are respectively the mass of the core rod and the sleeve (the inertia of viscoelastic material is ignored).

Using eq. (8), it can be derived that

$$\begin{aligned} &\boldsymbol{\Lambda} = G^{\infty}\bar{\boldsymbol{\Lambda}} = 2cG^{\infty}, \\ &\boldsymbol{Q} = G^{\infty}\bar{\boldsymbol{Q}}\bar{\boldsymbol{\Lambda}} = 2cG^{\infty}\begin{Bmatrix} \sqrt{2} \\ -\sqrt{2} \end{Bmatrix}, \quad \text{with} \quad c = \frac{2\pi R_2 L}{R_2 - R_1}. \end{aligned} \tag{10}$$

So, according to eq. (7), the coefficient matrices are

$$\hat{\boldsymbol{M}} = \begin{bmatrix} m_c & & & \\ & m_s & & \\ & & 0 & \\ & & & 0 \end{bmatrix}, \quad \hat{\boldsymbol{C}} = cG^{\infty}\begin{bmatrix} 0 & & & \\ & 0 & & \\ & & \dfrac{2a_1}{b_1} & \\ & & & \dfrac{2a_2}{b_2} \end{bmatrix},$$

$$\hat{\boldsymbol{K}} = cG^{\infty}\begin{bmatrix} 1+a_1+a_2 & -(1+a_1+a_2) & -a_1\sqrt{2} & -a_2\sqrt{2} \\ -(1+a_1+a_2) & 1+a_1+a_2 & a_1\sqrt{2} & a_2\sqrt{2} \\ -a_1\sqrt{2} & a_1\sqrt{2} & 2a_1 & 0 \\ -a_2\sqrt{2} & a_2\sqrt{2} & 0 & 2a_2 \end{bmatrix}. \tag{11}$$

We choose ZN-1 rubber as the viscoelastic material. Using the data at 30℃ given in ref. [16], the parameters of Biot model are fitted as those in Table 3.

4 Axial modal strain energy in Kagome truss

To keep the expense within the acceptable extent and main-

Table 3 Fitting parameters of Biot model for ZN-1 at 30℃

Parameter	G^{∞}	a_1	a_2	b_1	b_2
Value	5.0013×10^5	2.8438	35.6028	830.1878	13758

tain enough stiffness of the Kagome structure, only a very small portion of the rods in the planar Kagome truss will be replaced by the cylindrical dampers. As known, the location of the small number of cylindrical dampers will significantly influence the consequence of the modal damping in the Kagome structure. The approaches to an optimal placement of the dampers can be classified into two categories. One is to solve the problem of combinatory optimization directly. Various alternative techniques can be used like simulated annealing [17] and genetic algorithm [18]. But this approach is too expensive when the number of possible locations is very large. The other kind of approaches is to use effectiveness indices to quantify the fitness of different location. The fraction of modal elastic strain energy [19] of the elements in a structure is usually chosen as the index. This method is intuitive and can often get remarkable result even though which is not the most optimal one.

Since the rods in the planar Kagome truss are modeled by beam-like elements while the cylindrical dampers can be regarded as a kind of rod element that can not suffer bending or torsion moments, the fraction of axial modal strain energy should be used here.

The total modal elastic strain energy of the ith mode is written as

$$E_i = \frac{1}{2}\{\phi\}_i^{\mathrm{T}}[\boldsymbol{K}]\{\phi\}_i, \tag{12}$$

where $\{\phi\}_i$ is the mode shape of ith mode, and $[\boldsymbol{K}]$ is the global stiffness matrix of the structure.

The axial strain energy of element j at mode i is denoted by

$$E_{ij}^a = \frac{EA}{2L^3}\left(\Delta x_j^1 \Delta\phi_{ij}^1 + \Delta x_j^2 \Delta\phi_{ij}^2 + \Delta x_j^3 \Delta\phi_{ij}^3\right)^2, \tag{13}$$

where L is the length of the truss element. Δx_j^k, k=1, 2, 3 are the components of node coordinate differences of element j. $\Delta\phi_{ij}^k$, k=1, 2, 3 are the component of node differences in the mode shapes $\{\phi\}_i$ of element j. The fraction of axial modal strain energy (or FAMSE, in short) of element j in mode i is then define as

$$\delta_{ij} = \frac{E_{ij}^a}{E_i}. \tag{14}$$

This quantity will be used as the effective index to determine which rods will be replaced by the dampers.

5 Vibration control of the Kagome structure

5.1 Vibration control of single mode

For modes 1 to 3, we choose 8 rods in the planar Kagome truss, which take only 0.51% of the total rods in the planar Kagome truss, with significant FAMSE to be replaced by the cylindrical dampers. For the first mode and second mode, the allocations of dampers are the same. The placements of the dampers for first three modes are shown in Figure 5. As can be seen, the dampers are all located near the constrained boundaries.

Through the complex model analysis, the complex eigenvalue λ can be calculated as

$$\lambda = -\xi\omega_n \pm j\omega_n\sqrt{1-\xi^2}. \tag{15}$$

Then the natural frequency ω_n and damping factor ξ of each mode can be obtained from λ. The results are listed in Table 4 for the vibration control on modes 1 and 2 and in Table 5 for that on mode 3. Some conclusions can be drawn

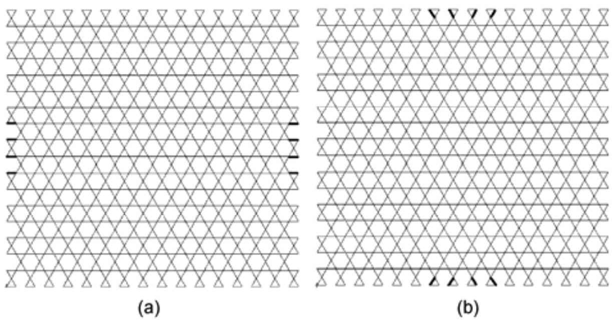

Figure 5 The locations of the dampers in the design for different controlled modes. The heavy solid line segments represent the dampers. (a) For modes 1 and 2; (b) for mode 3.

Table 4 The results of complex modal analysis under the dampers placement design for modes 1 and 2

Mode #	Damping ratio	Increment of damping ratio	Frequency (Hz)	Decrement of frequency (%)
1	0.0300	0.0200	112	5.08
2	0.0311	0.0211	208	4.59
3	0.0118	0.0016	231	0.43

Table 5 The results of complex modal analysis under the dampers placement design for mode 3

Mode #	Damping ratio	Increment of damping ratio	Frequency (Hz)	Decrement of frequency (%)
1	0.0243	0.0143	113	4.24
2	0.0104	0.0004	217	0.46
3	0.0309	0.0207	222	4.31

from the results.

i) The fraction of axial modal strain energy method is considerably effective. Among all the three cases for the single mode vibration control, the damping ratio has been significantly increased for the controlled mode (it is the largest one) through replacement of only 0.51% of the total Kagome truss rods by the cylindrical dampers.

ii) When the damping ratio raises in this way, the corresponding frequency always has a little drop (referring to Table 2 for reference). The raise of the damping ratio is at the some cost of losing stiffness of the structure.

5.2 Broad-bandwidth vibration control

In practice, the structure is often subjected to the excitation with broad-bandwidth frequencies. So it is necessary to develop a vibration control approach that can suppress the vibration containing several modes simultaneously.

Below FAMSE is further used as the index to optimize the location of the dampers. The goal is to search the rods in the planar Kagome truss with remarkably large FAMSE at all the controlling modes. The excitation frequency band width in the case studied here contains first six modes. In this paper the number of dampers used is 20, which takes only 1.26% of the total rods in the planar Kagome truss. The total FAMSE in mode i of the N chosen elements (rods) is defined as

$$\delta_i = \sum_j^{20} \delta_{ij}, \quad i=1\text{–}6. \tag{16}$$

Let $e=\min\delta_i$ (i varies from 1 to 6) indicate the minimum of the total FAMSE from mode 1 to mode 6 for the 20 chosen rods. The target of the optimization is to maximize e by selecting different combination of 20 rods.

To simplify the optimization procedure, we define a new total FAMSE of all the six modes in element j as

$$\delta_j = \sum_i^{6} \delta_{ij}. \tag{17}$$

In the optimization procedure, 100 elements that have the top largest δ_j are first determined from 1584 truss rods in the planar Kagome truss. Then, 20 elements will be selected from the 100 elements. Due to symmetrical placement of the dampers, the computation of the optimization search can be significantly reduced. That is, selection of 5 locations of elements from 25 candidates, namely C_{25}^5. The optimal positions of the dampers are shown in Figure 6(a). For the purpose of comparison, the effect of vibration control with the dampers placed in a relatively uniform style, as shown by Figure 6(b), is also calculated.

The results of the damping ratios and the natural frequencies of the Kagome structure with dampers through complex modal analysis are shown in Table 6. It is seen that the damping ratios of modes 1 to 6 have been considerably increased. The optimized placement of the dampers using FAMSE method achieves better results in comparison with those by a relatively uniform placement of the dampers (compare data in Tables 6(a) and (b)). The later achieve a

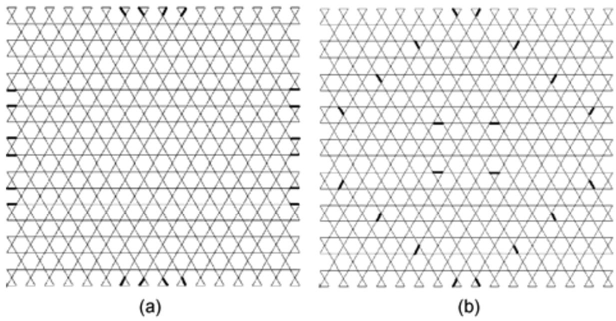

Figure 6 (a) The position of the dampers using FAMSE method; (b) the positions of the dampers in a relatively uniform style. The heavy solid line segments represent the dampers.

Table 6 The results of complex modal analysis with the dampers

(a) Placement of dampers using FAMSE method

Mode #	Damping ratio	Increment of damping ratio	Frequency (Hz)	Decrement of frequency (%)
1	0.0460	0.0360	106	10.17
2	0.0329	0.0229	207	5.05
3	0.0382	0.0281	218	6.03
4	0.0260	0.0141	310	2.52
5	0.0365	0.0237	343	3.65
6	0.0321	0.0186	376	3.34

(b) Placement of dampers in a relatively uniform style

Mode #	Damping ratio	Increment of damping ratio	Frequency (Hz)	Decrement of frequency (%)
1	0.0243	0.0143	104	11.86
2	0.0201	0.0101	201	7.80
3	0.0226	0.0124	211	9.05
4	0.0235	0.0116	285	10.38
5	0.0258	0.0130	323	9.27
6	0.0248	0.0113	358	7.97

larger increment of damping ratios through the greater reduction of the stiffness of the Kagome structure with a sharp decrease of natural frequencies in all the six modes.

To validate this passive vibration control approach, responses of the Kagome structure during the excitation of vertically downward distributed white noise load on the solid face sheet are computed. The white noise is with finite bandwidth of 2000 Hz. The single-side power spectrum density is 10 N^2/Hz.

The lateral responses of the Kagome structure, observed at the point shown in Figure 2(a), in the cases without dampers and with the dampers in placement as shown in Figure 6(a) and (b). respectively are drawn in Figure 7(a). It is found that the response amplitudes are considerably reduced with the installation of dampers in the structure. The response amplitudes in the case with optimized placement of the dampers are even smaller than those in the case of the relatively uniform placement of the dampers.

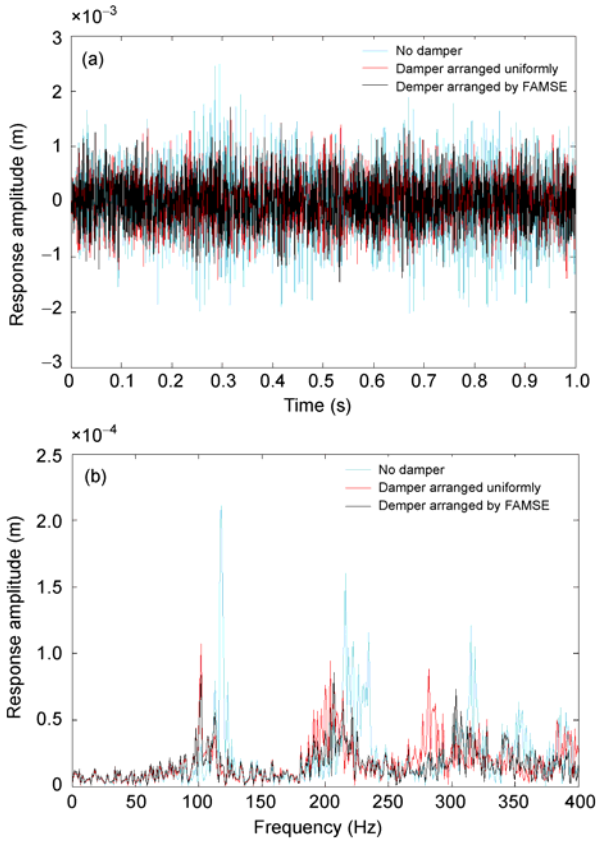

Figure 7 (a) The time history of response under the excitation of white noise; (b) spectra of responses.

From the spectrum of the responses shown in Figure 7(b), the effectiveness of the passive vibration control method proposed in this paper can be easily seen. The value of the percentage of reduction of the response amplitudes can be read from Table 7. The advantage of the optimal placement of the dampers over the relatively uniform placement of the dampers can also be observed. Furthermore, the shift of the resonance peaks is detectable (see Figure 7(b)) due to the replacement of the truss rods by the dampers. However, the reduction of the structure stiffness is smaller in the optimal placement of the dampers.

6 Conclusions

In this paper the realization of passive vibration control in a Kagome based high authority shape morphing structure is studied. The character of the Kagome structure that axial deformation of the rods in the planar Kagome truss can cause lateral deformation of the sandwich plate is utilized. Through the replacement of a very small portion of the rods in the planar Kagome truss by the cylindrical viscoelastic dampers, effective enhancement of the damping property of the Kagome structure is achieved. It is shown that the fraction of axial modal elastic strain energy of the rods in the planar Kagome truss is an effectiveness index to optimize the position of the dampers. The numerical results of the single mode vibration control and the broad-bandwidth vibration control method have shown significant increase in the damping ratios and the reduction of the response amplitudes of the Kagome structure.

The present approach for the lateral vibration control of a sandwich plate is quite different from the previous vibration control methods, such as the constrained layer damping, which usually take use of the bending induced shear deformation of the viscoelastic materials. The tension-compression induced shear deformation of the viscoelastic materials is utilized by using the feature of the Kagome structure to enhance the structural damping. The efficiency of this method in the increment of damping should be compared with the traditional methods quantitatively in the future. Furthermore, the replacement of the rods in planar Kagome truss by the cylindrical viscoelastic dampers with low-stiffness will cause some reduction of the structural stiffness. So the enhancement of structural damping must be balanced against the reduction of the structural stiffness in practice.

Table 7 Percentages of decreases of resonance peaks by different ways of the placement of the dampers

Resonance peak #	1	2	3	4	5	6
Damper placement by FAMSE method	60.2	46.5	44.5	39.3	37.1	61.3
Damper placement in relatively uniform style	49.2	41.3	37.8	27.2	21.4	15.7

The work was supported by the National Basic Research Program of China ("973" Project) (Grant No. 2006CB601206).

1 Dos Santos e Lucato S L, Wang J, Maxwell P, et al. Design and demonstration of a high authority shape morphing structure. Int J Solids Struct, 2004, 41: 3521–3543
2 Hutchinson R G, Wicks N, Evans A G, et al. Kagome plate structures for actuation. Int J Solids Struct, 2003, 40: 6969–6980
3 Wang J, Nausieda A, Dos Santos e Lucato S L, et al. Twisting of a high authority morphing structure. Int J Solids Struct, 2007, 44: 3076–3099
4 Yan M J, Dowell E H. Governing equations of vibrating constrained-layer damping sandwich plates and beams. ASME J Appl Mech, 1972, 39: 1041–1046
5 Woody S C, Smith S T. Damping of a thin-walled honeycomb structure using energy absorbing foam. J Sound Vib, 2006, 291: 491–502
6 Lü G. Combined Integrated Vibration Control for Truss Structures and The Application in Space Structures (In Chinese). Dissertation of Doctoral Degree. Xi'an: Xi'an Jiaotong University, 1998
7 Christensen R M. Theory of Viscoelasticity: An Introduction. New York: Academic Press, 1982
8 Johnson C D, Kienholz D A. Finite element prediction of damping in structures with constrained viscoelastic layers. AIAA J, 1982, 20: 1284–1290
9 Bagley R L, Torvik P J. Fractional calculus—a different approach to the analysis of viscoelastically damped structures. AIAA J, 1983, 21: 741–748
10 Lesieutre G A, Mingori D L. Finite element modeling of frequency-dependent material properties using augmented thermodynamic fields. AIAA J Guid Control Dynam, 1990, 13: 1040–1050
11 Lesieutre G A, Bianchini E. Time domain modeling of linear viscoelasticity using anelastic displacement fields. ASME J Vib Acoustics, 1995, 117: 424–430
12 Golla D F, Hughes P C. Dynamics of viscoelastic structures—A time domain finite element formulation. ASME J Appl Mech, 1985, 52: 897–906
13 Biot M A. Variation principles in irreversible thermodynamics with application to viscoelaticity. Phys Rev, 1955, 97: 1463–1469
14 McTavish D J. Time-domain response of damped linear structures using first-order GHM finite elements. T Can Soc Mech Eng, 2004, 28: 603–629
15 Zhang J, Zheng G T. The Biot model and its application in viscoelastic composite structures. J Vib Acoust, 2007, 129: 533–540
16 Chen Q. The Dynamic Analysis of Composite Structure of Viscoelastic Material (In Chinese). Dissertation of Doctoral Degree. Nanjing: Nanjing University of Aeronautics & Astronautics, 1987
17 Chen G S, Bruno R J, Salama M. Optimal placement of active/passive members in truss structures using simulated annealing. AIAA J, 1991, 29: 1327–1334
18 Bishop J A, Striz A G. On using genetic algorithms for optimum damper placement in space trusses. Struct Multidisc Optim, 2004, 28: 136–145
19 Preumont A, Dufour J P, Malekian C. Active damping by a local force feedback with piezoelectric actuators. In: Structural Dynamics and Materials Conference, American, 1991. 1879–1887